7868 J. Med. Chem. 2009, 52, 7868–7872
DOI: 10.1021/jm900576g

Journal of Medicinal Chemistry
Brief Article

High Lipophilicity of meta Mn(III) *N*-Alkylpyridylporphyrin-Based Superoxide Dismutase Mimics Compensates for Their Lower Antioxidant Potency and Makes Them as Effective as Ortho Analogues in Protecting Superoxide Dismutase-Deficient *Escherichia coli*

Ivan Kos,[†,∥] Ludmil Benov,[§] Ivan Spasojević,[‡] Júlio S. Rebouças,[†,⊥] and Ines Batinić-Haberle*[,†]

[†]*Department of Radiation Oncology and* [‡]*Department of Medicine, Duke University Medical School, Durham, North Carolina 27710, and* [§]*Department of Biochemistry, Faculty of Medicine, Kuwait University, Safat 13110, Kuwait.* [∥] *Present address: Faculty of Pharmacy and Biochemistry, University of Zagreb, A. Kovacica 1, 10 000 Zagreb, Croatia.* [⊥] *Present Address: Departamento de Química, CCEN, Universidade Federal da Paraíba, Caixa Postal 5093, João Pessoa, PB, 58051-970, Brazil.*

Received May 5, 2009

Lipophilicity/bioavailibility of Mn(III) *N*-alkylpyridylporphyrin-based superoxide dismutase (SOD) mimics has a major impact on their in vivo ability to suppress oxidative stress. Meta isomers are less potent SOD mimics than ortho analogues but are 10-fold more lipophilic and more planar. Enhanced lipophilicity contributes to their higher accumulation in cytosol of SOD-deficient *Escherichia coli*, compensating for their lower potency; consequently, both isomers exert similar-to-identical protection of SOD-deficient *E. coli*. Thus meta isomers may be prospective therapeutics as are ortho porphyrins.

Introduction

Positively charged Mn(III) *N*-alkylpyridylporphyrins (Figure 1) display electrostatic and thermodynamic facilitation for the dismutation of superoxide ($O_2^{\bullet-}$) and reduction of peroxynitrite ($ONOO^-$).[1−4] Some members of the series are among the most potent catalytic scavengers of these reactive species with activity toward $O_2^{\bullet-}$ nearly the same as that of the superoxide dismutase (SOD) enzymes,[4] and reactivity toward $ONOO^-$, k_{red} exceeding 10^7 M^{-1} s^{-1}.[3] Reactive species are widely viewed as signaling molecules controlling cellular transcriptional activity.[5] Thus, inhibition of the activation of redox-active transcription factors such as AP-1,[6] NF-κB,[7,8] and HIF-1α,[9−11] presumably via scavenging of reactive species by some members of the series was detected. Mn porphyrins, such as MnTE-2-PyP, MnTnHex-2-PyP, and MnTDE-2-ImP,[a] effectively attenuate oxidative stress in animal models of cancer,[6,9−11] central nervous system disorders,[8] radiation injury,[12] diabetes,[7,13] morphine tolerance,[14] ischemia/reperfusion injuries,[16] etc. Recent data, however, has hinted that factors other than redox-based antioxidant potency such as lipophilicity, size, and the overall geometry and conformational flexibility of the Mn porphyrins (MnP) should play also a significant role in their design and activity.[4,15,17]

In our seminal work published in 1998,[18] the magnitude and the importance of the lipophilicity for the in vivo SOD-like efficacy of MnP as well as the remarkable gain in lipophilicity (at the expense of activity) by the mere shift of the alkyl group from an ortho onto a meta position could only have been retrospectively speculated. Recently, we were able to overcome the methodological difficulties associated with the determination of the partition coefficients between *n*-octanol and water, P_{OW}. The P_{OW}, as opposed to TLC retention factor, R_f, is a common and practical indicator of drug lipophilicity that allows comparison of MnP to other drugs of similar target (Table 1).[17] We observed that, whereas R_f is linearly related to log P_{OW}, small differences in R_f translate into considerable difference in log P_{OW}.[17] We further showed that a ∼10-fold gain in lipophilicity is achieved by either (1) moving the alkyl groups on meso pyridyl substituents from ortho to meta positions, or (2) by increasing the length of alkyl chains by one CH_2 group (Table 1).[17] Thus, MnTnHex-2-PyP and MnTnOct-2-PyP are, respectively, ∼13000- and ∼460000-fold more lipophilic than MnTE-2-PyP. Whereas these compounds share roughly the same antioxidant capacity (as given by their log k_{cat} values), the 120- and 3000-fold increase in in vivo efficacy of MnTnHex-2-PyP[12,16,20,22,23] and MnTnOct-2-PyP[20,21] (relative to MnTE-2-PyP) in animal and cellular models of oxidative stress seems to be due, at least in part, to their increased lipophilicity and therefore increased cellular accumulation. Among several different classes of metal compounds studied (Mn cyclic polyamines, Mn salens, different MnP and $MnCl_2$ as a control), only MnTnHex-2-PyP protects ataxia telangiectasia cells against radiation damage in a first study to show that both bioavailability and antioxidant capacity are essential for in vivo drug efficacy.[23] In a rabbit model of cerebral palsy MnTnHex-2-PyP, and not MnTE-2-PyP, rescued puppies.[23] Due to the exceptional antioxidant potential of ortho isomeric Mn *N*-alkylpyridylporphyrins in dismuting $O_2^{\bullet-}$ and reducing $ONOO^-$, we[1−4] and others[24] have been extensively studying them and analogues of ortho-substituted corroles.[25]

*To whom correspondence should be addressed. Phone: 919-684-2101. Fax: 919-684-8718 E-mail: ibatinic@duke.edu. Address: Department of Radiation Oncology, Duke University Medical Center, Research Drive 281b/285 MSRB I, Box 3455, Durham, NC 27710.

[a] Abbreviations (charges are omitted throughout text): MnTalkyl-2(or 3)-PyP^{5+}, Mn(III) *meso*-tetrakis(*N*-alkylyridinium-2 or 3-yl)porphyrin, alkyl being methyl (M, AEOL10112), ethyl (E, AEOL10113), *n*-propyl (nPr), *n*-butyl (nBu), *n*-hexyl (nHex), *n*-heptyl (nHep), *n*-octyl (nOct), 2 and 3 relate to ortho and meta isomers, respectively; MnTDE-2-ImP, Mn(III) tetrakis(*N*,*N*′-diethylimidazolium-2-yl)porphyrin, AEOL10150; R_f = porphyrin path/solvent path, thin-layer chromatographic (TLC) retention factor.

 Published on Web 07/21/2009

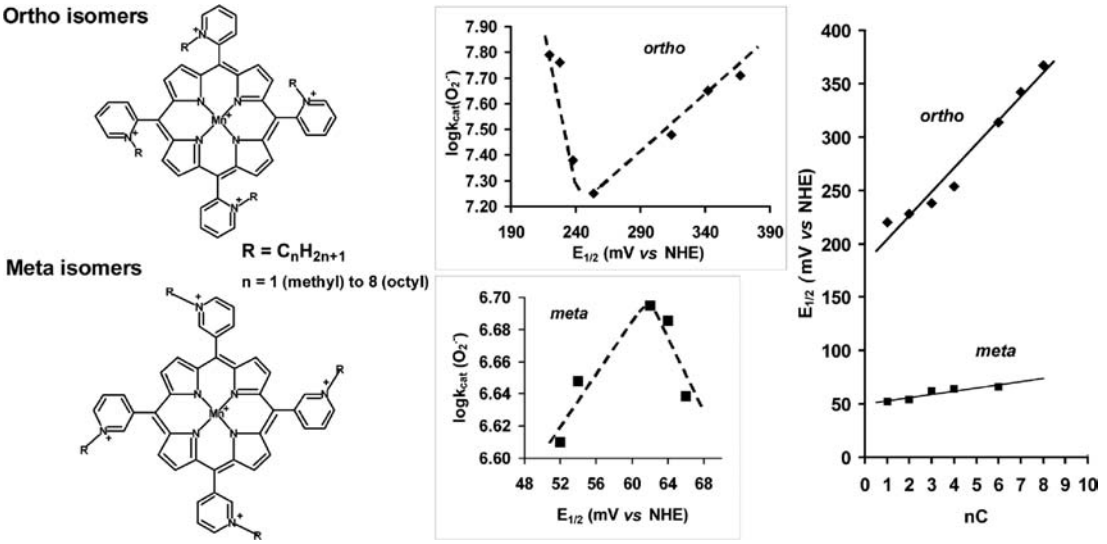

Figure 1. Structures of meta and ortho Mn(III) *N*-alkylpyridylporphyrins and the relationships between the log k_{cat} ($O_2^{\bullet-}$) [at (25 ± 1) °C, k_{cat} in $M^{-1}s^{-1}$] and $E_{1/2}$ ($Mn^{III}P/Mn^{II}P$ redox couple) and $E_{1/2}$ and the number of carbon atoms (nC) in the alkyl groups (R) of isomers.

Table 1. Lipophilicity Expressed as TLC Retention factor, R_f (Sigma/Aldrich Silica Gel Plates with KNO_3-Saturated H_2O:H_2O:acetonitrile = 1:1:8)[17] and Partition between *n*-Octanol and Water, P_{OW},[17] k_{cat} for $O_2^{\bullet-}$ Dismutation (at (25 ±1)°C, 0.05 M Phosphate Buffer, pH 7.8) (Refs 2, 18, 19, and This Work) and the Metal-Centered Reduction Potential for $Mn^{III}P/Mn^{II}P$ Redox Couple, $E_{1/2}$, in mV vs NHE (in 0.05 M Phosphate Buffer, pH 7,8, 0.5 mM MnP, 0.1 M NaCl) (Refs 2, 18, 19, and This Work)

porphyrin	R_f	log P_{OW}	$E_{1/2}$	log k_{cat}
MnTM-2-PyP	0.03	−7.86	+220	7.79
MnTE-2-PyP	0.06	−6.89	+228	7.76
MnTnPr-2-PyP	0.11	−5.93	+238	7.38
MnTnBut-2-PyP	0.19	−5.11	+254	7.25
MnTnHex-2-PyP	0.38	−2.76	+314	7.48
MnTnHep-2-PyP	0.46	−2.10	+342	7.65
MnTnOct-2-PyP	0.49	−1.24	+367	7.71
MnTM-3-PyP	0.05	−6.96	+52	6.61
MnTE-3-PyP	0.10	−5.98	+54	6.65
MnTnPr-3-PyP	0.22	−5.00	+62	6.69
MnTnBut-3-PyP	0.40	−4.03	+64	6.69
MnTnHex-3-PyP	0.55	−2.06	+66	6.64

The ~10-fold increase in the lipophilicity of the meta as compared to ortho isomers may compensate for their inferior antioxidant potency, making them prospective therapeutics. Further, the rotational flexibility of the meta isomers when compared to conformational rigidity of the ortho isomers may affect favorably their cellular uptake and subcellular biodistribution. We thus decided to revisit meta isomers to better describe the factors that contribute to the in vivo efficacy of these seemingly different MnP. For in vivo studies, we employed our simple and convenient $O_2^{\bullet-}$-specific model that relies on the aerobic growth of SOD-deficient *Escherichia coli*. Thus far, it has always been a reliable predictor of a prospective drug candidate.[18,20]

Results and Discussion

Two new meta isomers, MnTE-3-PyP and MnTnPr-3-PyP, were synthesized and characterized by elemental analysis, UV/vis spectroscopy, ESI-MS, electrochemistry ($E_{1/2}$), lipophilicity (R_f and P_{OW}) and SOD-like activity (k_{cat}) (Table 1 and Table 1S of the Supporting Information). There are no significant differences in the UV/vis spectral properties of new compounds (see Experimental Section and Table 1S of the Supporting Information) relative to other meta analogues.[19] The ESI-MS spectral pattern, given in the Experimental Section, was similar to that described previously for the ortho methyl and ethyl analogues.[26] Elemental analyses (Experimental Section) are consistent with the hydrated species.

Dependence of the $Mn^{III}P/Mn^{II}P$ Reduction Potential ($E_{1/2}$) and the SOD Activity (k_{cat}) on the Number of C Atoms in the *N*-Alkylpyridyl Chains. The lengthening of the ortho alkyl groups influences dramatically solvation and stericity of the porphyrin, which, in turn, affects $E_{1/2}$ and k_{cat}, as previously discussed in detail.[19] Briefly, as the alkyl chain grows from one to eight carbon atoms, due to the increasingly less solvated, thus more exposed positive charges on pyridyls, the $E_{1/2}$ grows approximately linearly from +220 to +367 mV vs NHE (Table 1). However, the dependence of k_{cat} on the number of carbons reveals a delicate balance between two antagonistic factors: the increase of steric hindrance, i.e., crowding near the Mn site, which would decrease k_{cat}, and the increase of the $Mn^{III}P/Mn^{II}P$ reduction potential ($E_{1/2}$), which is a surrogate for the driving force of the electron transfer and would increase k_{cat}. Accordingly, k_{cat} first decreases from methyl to butyl as the steric hindrance to the approach of $O_2^{\bullet-}$ to the Mn site increases but then increases as the favorable thermodynamics for the dismutation reaction ($E_{1/2}$) predominates (Table 1, Figure 1).[19] The maximum change in $E_{1/2}$ is 147 mV and in k_{cat} 0.54 log units (Table 1).

When the alkyl side chains are located in the meta positions, farther from the porphyrin core, free rotation of the pyridyl groups is allowed and the steric and the solvation effects are thus much less pronounced. Consequently, the maximum change in $E_{1/2}$ for the meta series is only 14 mV and for k_{cat} only 0.08 log units (Figure 1). As the alkyl chain lengthens, $E_{1/2}$ continuously increases (Table 1, Figure 1). For small alkyl side chains, the favorable thermodynamics dominates and an initial small increase in k_{cat} is observed. As the alkyl chains lengthen further (from *n*-butyl on), the steric hindrance prevails over the increase in $E_{1/2}$ and k_{cat} starts to decrease. As a result of such trends, the SOD activity of some members of the meta series is close to the respective analogues in the ortho series; this happens for example for the *n*-propyl and *n*-butyl compounds where the SOD activities of the respective ortho and meta isomers approach each other

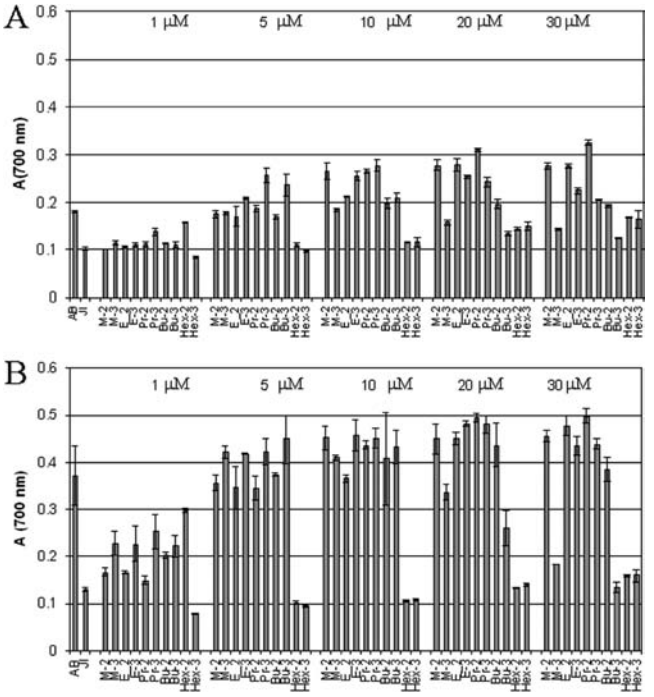

Figure 2. Aerobic growth of SOD-deficient *E. coli* JI 132 in five-amino-acid minimal medium (absorbance at 700 nm) in the presence of ortho (2) and meta (3) analogues shown here at 14 (A) and 18 h (B) of growth. The growth of SOD-proficient *E. coli* AB1157 is shown also. Bars represent mean ± SE.

(Figure 1,Table 1). It is worthwhile noting, however, that while the k_{cat} of the ortho *n*-propyl and ortho *n*-butyl compounds are only about 4.9- and 3.6-fold higher than that of their meta analogues, the lipophilicity of the meta isomers remains 10-fold bigger throughout the series (Table 1).[17] Therefore, due to the interplay of antioxidant potency and lipophilicity, some members of the meta series may be of identical or higher efficacy than ortho isomers in in vivo models of oxidative stress. To explore such an assumption, we studied here the accumulation and the efficacy of both isomeric series in protecting SOD-deficient *E. coli*.

SOD-Deficient *E. coli* (JI132) Growth. Efficacy of MnP. The JI132 strain lacks two cytoplasmic SODs, FeSOD and MnSOD, and thus displays phenotypic defects attributable to the damage of important cellular components by superoxide.[27−30] Among those phenotypic deficiencies is the inability to grow aerobically in minimal glucose medium.[29] Only compounds that are potent, cell-permeable SOD mimics, can exert protection, thus restoring the aerobic growth in minimal medium.[31] Our data show that ortho and meta isomers protect SOD-deficient *E. coli* with nearly equal efficacy (Figure 2). The meta and ortho ethyl, *n*-propyl, and *n*-butyl porphyrins appear of nearly identical efficacy at higher concentrations (10 and 20 μM), but meta analogues and the more lipophilic *n*-propyl and *n*-butyl porphyrins are more efficacious than ortho analogues at lower concentrations (1 and 5 μM), presumably due to their faster cellular uptake (Figure 2 and Figure 1S of the Supporting Information). The structural flexibility of the meta isomers, which allows them to change their shape and size while crossing the membranes, is difficult to quantify but likely contributes to their high efficacy. Our data suggest that the shorter and the more planar methyl analogue, MnTM-3-PyP, becomes somewhat less efficient at 10−30 μM levels presumably due to the enhanced unfavorable interactions with nucleic acids.[18] The more lipophilic MnTnBu-3-PyP, which also possesses significant surfactant character and can thus disturb the cell membranes, becomes toxic at concentrations ≥20 μM. MnTnHex-3-PyP of even stronger surfactant character is toxic at all concentrations studied; its ortho analogue is only slightly less toxic (Figure 2A); this is in agreement with our previous *E. coli* study on ortho Mn(III) *N*-alkylpyridylporphyrins.[18]

Toxicity of MnP to Wild-Type *E. coli*, AB1157. Further assessment of MnP toxicity was accomplished by monitoring their effect on the growth of AB1157, in complete, M9CA medium. None of the Mn porphyrins exerted toxicity at concentrations at which they protected the SOD-deficient JI132 strain (Supporting Information Figure 2S). At higher concentrations, however, the same trend in toxicity, as observed with the growth of JI132, was seen with AB1157 in M9CA medium. MnTM-3-PyP, and more so MnTnBu-3-PyP, exerted toxicity at ≥100 μM (Figure 2AS). Both hexyl analogues accumulate to the highest degree in cytosol and membranes (Figure 3) and exert toxicity at concentrations ≥1 μM (Figure 2BS). No toxicity of Mn porphyrins to AB1157 (alkyl = methyl to *n*-butyl) was observed in five-amino-acid minimal medium at 20 μM levels (Supporting Information Figure 3S).

Accumulation of Porphyrins. Accumulation of MnPs in cytosolic (Figure 3) and membrane fractions (Figure 5S of the Supporting Information) was assessed in both AB 1157 and JI132 *E. coli*. Both strains show similar MnP accumulation profile, but on average, the absolute uptake of MnPs is higher in the JI132 strain; this is clearly visible with the hexyl analogues and may be driven by a general *E. coli* attempt to accumulate nutrients or biologically relevant compounds that are neither produced within nor readily available. Because the SOD-deficient *E. coli* strain lacks two cytosolic superoxide dismutases, accumulation of SOD mimics in the cytosol is essential for protecting SOD-deficient mutant. The levels of porphyrins within cytosol and membrane (Figure 3 and Figure 5S of the Supporting Information) were quantified by using calibration curves for ortho and meta isomeric porphyrins, where area below the porphyrin Soret band was plotted vs porphyrin concentration (Figure 4S of the Supporting Information). Two major findings, depicted in Figure 3, are: (1) Compared to ortho analogues, meta isomers accumulate to significantly higher levels in the cytosol of both strains; due to the more planar structure (conformationally flexible) and higher lipophilicity they cross membrane more easily, which apparently overcomes the inferior thermodynamics of meta isomers for $O_2^{\bullet-}$ dismutation, contributing at least in part to their high efficacy in substituting for deficiency in both cytosolic SODs. Consequently, the efficacy of meta and ortho ethyl and *n*-propyl analogues in *E. coli* study are nearly identical. (2) Ortho and meta hexyl analogues, which possess strong micellar character, accumulate much more than any other porphyrin in cytosol and membranes (Figure 3 and Figure 5S of the Supporting Information), which seems to compromises membrane structure and its functions.

Although meta and para isomers have similar $E_{1/2}$ and SOD activity, the systematic experimentation with the para isomers has remained on hold. Because of their conformational flexibility, para isomers adopt planar structures and thus interact extensively with nucleic acids,[15] which not only results in high toxicity but also prevents the approach of

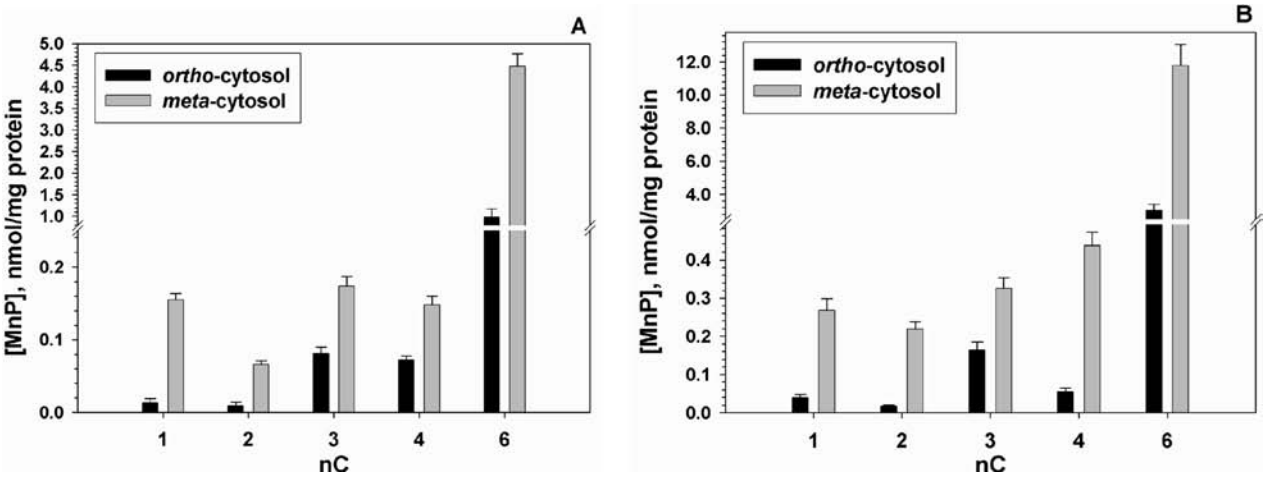

Figure 3. Accumulation of isomeric Mn(III) *N*-alkylpyridylporphyrins in cytosolic fractions of wild AB1157 (A) and SOD-deficient JI132 strain of *E. coli* (B). *E. coli* was incubated for 1 h with 5 μM MnP in M9CA medium. Bars represent mean ± SE. Accumulation in membranes is shown in Supporting Information, Figures 6S−9S.

superoxide to the Mn site;[15] this in turn suppresses their effects in protecting SOD-deficient *E. coli*.[15] The bulkiness of the ortho and meta isomers prevents such associations to a greater degree.[18] In light of the findings in the ortho and meta series described here, longer alkyl para analogues may be bulky enough to overcome possible nucleic acid intercalation and further studies with bulkier para isomers may thus be warranted.

Experimental Section

Experimental details are given in Supporting Information.

General. All chemicals are of highest purity and obtained from same commercial sources as indicated before.

Porphyrins. Elemental Analysis. (Atlantic MicroLab, Norcross, GA): H_2TE-3-PyPCl$_4\cdot 11H_2O$ ($C_{48}H_{72}N_8O_{11}Cl_4$) found: C, 53.82; H, 6.21; N, 10.89; Cl, 13.44; calcd: C, 53.43; H, 6.73; N, 10.39; Cl, 13.14. H_2TnPr-3-PyPCl$_4\cdot 16H_2O$ ($C_{52}H_{90}N_8O_{16}Cl_4$) found: C, 50.98; H, 5.78; N, 9.32; Cl, 11.75; calcd: C, 50.98; H, 7.40; N, 9.15; Cl, 11.58. MnTE-3-PyPCl$_5\cdot 8.5H_2O$ ($MnC_{48}H_{61}N_8O_{8.5}Cl_5$) found: C, 51.74; H, 5.13; N, 9.93; Cl, 16.53; calc: C, 51.56; H, 5.50; N, 10.02; Cl, 15.85. MnTnPr-3-PyPCl$_5\cdot 10H_2O$ ($MnC_{52}H_{76}N_8O_{10}Cl_5$) found: C, 51.39; H, 6.01; N, 9.22; Cl, 14.31; calc: C, 51.05; H, 6.43; N, 9.16; Cl, 14.49. Compounds are ≥99% pure.

Electrospray Ionization Mass Spectrometric Analyses. (ESI-MS) of 5 μM MnP in a H_2O−acetonitrile (1:1, v/v; containing 0.1% v/v HFBA) were done as described elsewhere.[26] The *m*/*z* peak assignments are consistent with the following species in the given order: $[MnT(alkyl)\text{-}3\text{-}PyP^{5+} + 2HFBA^-]^{3+}/3$), $[MnT(alkyl)\text{-}3\text{-}PyP^{5+} + HFBA^- - 2H^+]^{2+}/2$, $[MnT(alkyl)\text{-}3\text{-}PyP^{5+} + 2HFBA^- - H^+]^{2+}/2$, and $[MnT(alkyl)\text{-}3\text{-}PyP^{5+} + 3HFBA^-]^{2+}/2$. MnTE-3-PyPCl$_5$: found 404.7 499.3, 606.3, 713.6; calcd 404.6, 499.3, 499.3, 606.3, 713.5. MnTnPr-3-PyPCl$_5$: found 423.7, 527.5, −, 741.5; calcd 423.4, 527.6, 634.6, 741.6.

UV/Vis Spectra. Spectra were recorded in H_2O at room temperature (25 ± 1 °C). The λ(nm) of Soret bands and the corresponding molar absorptivities, ε (log values in parentheses) are: H_2TE-3-PyP 417.0(5.52); H_2TnPr-3-PyP 417.0(5.55); MnTE-3-PyP 460.0(5.19); MnTnPr-3-PyP 460.0 (5.14). Other absorption maxima and related ε are in Table 1S.

Cyclic Voltammetry. Cyclic voltammetry was performed as described elsewhere.[26]

SOD-Like Activity. Determination of the $k_{cat}(O_2^{\bullet -})$ using cyt *c* assay was performed as previously described in detail.[1,18]

In Vivo Studies. *E. coli* Growth. *E. coli* studies on SOD-deficient JI132 and wild type SOD-proficient strain AB1157 were performed as described.[31]

Accumulation of Mn Porphyrins in *E. coli*. The wild type AB1157 and JI132 were grown in flasks in 10 mL of M9CA medium to a density corresponding to $A_{700} \sim 0.6$. Five μM Mn porphyrins were then added, and the cells were kept on a shaker for additional 60 min. Cells were then rapidly washed with ice-cold PBS, resuspended to a total volume of 1.0 mL, and disrupted by sonication. Cytosolic and membrane fractions were separated by centrifugation. The membrane fractions were solubilized in 10% sodium dodecylsulfate for 24 h and then centrifuged at high speed to remove the unsolubilized material. Spectra were recorded and the absorbances of MnP in cytosolic and membrane fractions measured at their Soret bands.[19] Protein levels were measured by the Lowry method.[32] Details on the calculations of the accumulation of porphyrins in cytosolic and membrane fractions are given in Supporting Information along with related Figures 4S−9S.

Acknowledgment. I.K., J.S.R., and I.B.H. acknowledge support by NIAID U19AI67798-01 and W. H. Coulter Translation Partners Grant Program. I.S. thanks NIH/NCI DCCC for a core grant (5-P30-CA014236-33). L.B. thanks Kuwait University for grant MB03/07. We are grateful to HSC Research for a core facility grant GM01/01 and for the technical assistance of Milini Thomas.

Supporting Information Available: Experimental section; UV/vis characteristics of MnTE-3-PyP and MnTnPr-3-PyP; SOD-deficient E. coli growth as a function of MnP concentration; toxicity of MnP to AB1157 in M9CA medium; toxicity of MnP to AB1157 in five-amino-acid medium; calibration curve for calculation of MnP accumulation in *E. coli*; accumulation of MnP in membranes of *E. coli*; accumulation of MnTnPr-2(or 3)-PyP in cytosol and membranes of *E. coli*; accumulation of MnTnBu-2(or 3)-PyP in cytosol and membranes of *E. coli*; accumulation of MnTnPr-2(or 3)-PyP in cytosol and membranes *E. coli*; accumulation of MnTnPr-2(or 3)-PyP in whole *E. coli*. This material is available free of charge via the Internet at http://pubs.acs.org.

References

(1) Rebouças, J. S.; De Freitas-Silva, G.; Idemori, Y. M.; Spasojević, I.; Benov, L.; Batinić-Haberle, I. The impact of electrostatics in redox modulation of oxidative stress by Mn porphyrins. Protection of SOD-deficient *E. coli* via alternative mechanism where Mn porphyrin acts as a Mn-carrier. *Free Radical Biol. Med.* **2008**, *45*, 201–210.

(2) Batinić-Haberle, I.; Benov, L.; Spasojević, I.; Hambright, P.; Crumbliss, A. L.; Fridovich, I. The relationship between redox

potentials, proton dissociation constants of pyrrolic nitrogens, and in vitro and in vivo superoxide dismutase activities of manganese(III) and iron(III) cationic and anionic porphyrins. *Inorg. Chem.* **1999**, *38*, 4011–4022.
(3) Ferrer-Sueta, G.; Vitturi, D.; Batinić-Haberle, I.; Fridovich, I.; Goldstein, S.; Czapski, G.; Radi, R. Reactions of manganese porphyrins with peroxynitrite and carbonate radical anion. *J. Biol. Chem.* **2003**, *278*, 27432–27438.
(4) De Freitas-Silva, G.; Rebouças, J. S.; Spasojević, I.; Benov, L.; Idemori, Y. M.; Batinić-Haberle, I. SOD-like activity of Mn(II) β-octabromo-*meso*-tetrakis(*N*-methylpyridinium-3-yl)porphyrin equals that of the enzyme itself. *Arch. Biochem. Biophys.* **2008**, *477*, 105–112.
(5) Halliwell, B.; Gutterdige J. M. C. *Free Radicals in Biology and Medicine Biosciences*; Oxford University Press: New York, 2007.
(6) Zhao, Y.; Chaiswing, L.; Oberley, T. D.; Batinić-Haberle, I.; St. Clair, W.; Epstein, C. J.; St. Clair, D. A mechanism-based antioxidant approach for the reduction of skin carcinogenesis. *Cancer Res.* **2005**, *I*, 1401–1405.
(7) Tse, H.; Milton, M. J.; Piganelli, J. D. Mechanistic analysis of the immunomodulatory effects of a catalytic antioxidant on antigen-presenting cells: Implication for their use in targeting oxidation/reduction reactions in innate immunity. *Free Radical Biol. Med.* **2004**, *36*, 233–47.
(8) Sheng, H.; Sakai, H.; Yang, W.; Fukuda, S.; Salahi, M.; Day, B. J.; Huang, J.; Paschen, W.; Batinić-Haberle, I.; Crapo, J. D.; Pearlstein, R. D.; Warner, D. S. Sustained treatment is required to produce long-term neuroprotective efficacy from a metalloporphyrin catalytic antioxidant in focal cerebral ischemia, *Free Radical Biol. Med.* **2009**, in press.
(9) Moeller, B. J.; Cao, Y.; Li, C. Y.; Dewhirst, M. W. Radiation activates HIF-1 to regulate vascular radiosensitivity in tumors: Role of oxygenation, free radicals and stress granules. *Cancer Cell* **2005**, *5*, 429–441.
(10) Rabbani, Z. N.; Spasojević, I.; Zhang, X.; Moeller, B. J.; Haberle, S.; Vasquez-Vivar, J.; Dewhirst, M. W.; Vujaskovic, Z.; Batinić-Haberle, I. Anti-angiogenic action of redox modulating Mn(III) ortho tetrakis *N*-ethylpyridyl porphyrin, MnTE-2-PyP^{5+} via suppressing oxidative stress in a mouse model of breast tumor. *Free Radical Biol. Med.* **2009**, published online, DOI:10.1016/j.freeradbiomed.2009.07.001.
(11) Moeller, B. J.; Batinić-Haberle, I.; Spasojević, I.; Rabbani, Z. N.; Anscher, M. S.; Vujaskovic, Z.; Dewhirst, M. W. A manganese porphyrin superoxide dismutase mimetic enhances tumor radioresponsiveness. *Int. J. Radiat. Oncol., Biol., Phys.* **2005**, *63*, 545–552.
(12) Gauter-Fleckenstein, B.; Fleckenstein, K.; Owzar, K; Jian, C.; Batinić-Haberle, I.; Vujaskovic, Z. Comparison of two Mn porphyrin-based mimics of superoxide-dismutase (SOD) in pulmonary radioprotection. *Free Radical Biol. Med.* **2008**, *44*, 982–989.
(13) Piganelli, J. D.; Flores, S. C.; Cruz, C.; Koepp, J.; Young, R.; Bradley, B.; Kachadourian, R.; Batinić-Haberle, I.; Haskins, K. A metalloporphyrin superoxide dismutase mimetic (SOD mimetic) inhibits autoimune diabetes. *Diabetes* **2002**, *51*, 347–355.
(14) Batinić-Haberle, I.; Ndengele, M. M.; Cuzzocrea, S.; Rebouças, J. S.; Spasojević, I.; Salvemini, D. Lipophilicity is a critical parameter that dominates the efficacy of metalloporphyrins in blocking morphine tolerance through peroxynitrite-mediated pathways. *Free Radical Biol. Med.* **2009**, *46*, 212–219.
(15) Rebouças, J. S.; Spasojević, I.; Tjahjono, D. H.; Richaud, A.; Mendez, F.; Benov, L.; Batinić-Haberle, I. Redox modulation of oxidative stress by Mn porphyrin-based therapeutics: The effect of charge distribution. *J. Chem. Soc., Dalton Trans.* **2008**, 1233–1242.
(16) Saba, H.; Batinić-Haberle, I.; Munusamy, S.; Mitchell, T.; Lichti, C.; Megyesi, J.; MacMillan-Crow, L. A. Manganese porphyrin reduces renal injury and mitochondrial damage during ischemia/reperfusion. *Free Radical Biol. Med.* **2007**, *42*, 1571–1578.
(17) Kos, I.; Rebouças, J. S.; De Freitas-Silva, G.; Salvemini, D.; Vujaskovic, Z.; Dewhirst, M. W.; Spasojević, I.; Batinić-Haberle, I. The effect of lipophilicity of porphyrin-based antioxidants. Comparison of ortho and meta isomers of Mn(III) *N*-alkylpyridylporphyrins. *Free Radical Biol. Med.* **2009**, *47*, 72–78.
(18) Batinić-Haberle, I.; Benov, L.; Spasojević, I.; Fridovich, I. The ortho effect makes manganese (III) *meso*-tetrakis(*N*-methylpyridinium-2-yl)porphyrin (MnTM-2-PyP) a powerful and potentially useful superoxide dismutase mimic. *J. Biol. Chem.* **1998**, *273*, 24521–24528.
(19) Batinić-Haberle, I.; Spasojević, I.; Stevens, R. D.; Hambright, P.; Fridovich, I. Manganese(III) *meso*-tetrakis-*ortho*-*N*-alkylpyridylporphyrins. Synthesis, characterization and catalysis of $O_2^{\bullet-}$ dismutation. *J. Chem. Soc., Dalton Trans.* **2002**, 2689–2696.
(20) Okado-Matsumoto, A.; Batinić-Haberle, I.; Fridovich, I. Complementation of SOD-deficient *Escherichia Coli* by manganese porphyrin mimics of superoxide dismutase activity. *Free Radical Biol. Med.* **2004**, *37*, 401–10.
(21) Wise-Faberowski, L.; Warner, D. S.; Spasojević, I.; Batinić-Haberle, I. The effect of lipophilicity of Mn (III) *ortho*-*N*-alkylpyridyl- and di-*ortho*-*N*,*N*′-imidazolylporphyrins in two in vitro models of oxygen and glucose deprivation-induced neuronal death. *Free Radical Res.* **2009**, *43*, 329–339.
(22) Pollard, J.; Rebouças, J. S.; Durazo, A.; Kos, I.; Fike, F.; Panni, M.; Gralla, E. B.; Valentine, J. S.; Batinić-Haberle, I.; Gatti, R. A. Radioprotective effects of manganese-containing superoxide dismutase mimics on ataxia telangiectasia cells. *Free Radical Biol. Med.* **2009**, *47*, 250–260.
(23) Tan, S.; Batinić-Haberle, I.; MnTnHex-2-PyP in rabbit cerebral palsy model, unpublished.
(24) Szabó, C.; Mabley, J. G.; Moeller, S. M.; Shimanovich, R.; Pacher, P.; Virag, L.; Soriano, V. G.; van Duzer, J. H.; Williams, W.; Salzman, A. L.; Groves, J. T. Pathogenic role of peroxynitrite in the development of diabetes and diabetic vascular complications: Studies with FP15, a novel potent peroxynitrite decomposition catalyst. *Mol. Med.* **2002**, *8*, 571–580.
(25) Saltsman, I.; Botoshansky, M.; Gross, Z. Facile synthesis of *ortho*-pyridyl-substituted corroles and molecular structures of analogues porphyrins. *Tetrahedron Lett.* **2008**, *49*, 4163–4166.
(26) Rebouças, J. S.; Spasojević, I.; Batinić-Haberle, I. Quality of Mn-porphyrin-based SOD mimics and peroxynitrite scavengers for preclinical mechanistic/therapeutic purposes. *J. Pharm. Biomed. Anal.* **2008**, *48*, 1046–1049.
(27) Imlay, J. A. Cellular defenses against superoxide and hydrogen petoxide. *Annu. Rev. Biochem.* **2008**, *77*, 755–776.
(28) Imlay, J. A. Pathways of oxidative damage. *Annu. Rev. Microbiol.* **2003**, *57*, 395–418.
(29) Carlioz, A.; Touati, D. Isolation of superoxide dismutase mutants in *Escherichia coli*: is superoxide dismutase necessary for aerobic life?. *EMBO* **1986**, *5*, 623–630.
(30) Messner, K. R.; Imlay, J. A. The identification of primary sites of superoxide and hydrogen peroxide formation in the aerobic respiratory chain and sulfite reductase complex of *Escherichia coli*. *J. Biol. Chem.* **1999**, *274*, 10119–10128.
(31) Batinić-Haberle, I.; Cuzzocrea, S.; Rebouças, J. S.; Ferrer-Sueta, G.; Emanuela Mazzon, E.; Di Paola, R.; Radi, R.; Spasojević, I.; Benov, L.; Salvemini, D. Pure MnTBAP selectively scavenges peroxynitrite over superoxide: comparison of pure and commercial MnTBAP samples to MnTE-2-PyP in two different models of oxidative stress injuries, SOD-specific *E. coli* model and carrageenan-induced pleurisy. *Free Radical Biol. Med.* **2009**, *46*, 192–201.
(32) Lowry, O. H.; Rosebrough, N. J.; Farr, A. L.; Randall, R. J. Protein measurement with the folin phenol reagent. *J. Biol. Chem.* **1951**, *193*, 265–275.